THE CALC-ALKALINE MONTE CAPO STELLA DYKES IN THE OPHIOLITIC UNIT OF THE ELBA ISLAND (ITALY): GEOLOGICAL SETTING AND COMPOSITIONAL CHARACTERIZATION

Enrico Pandeli*,°,✉, Alba P. Santo*,°, Monica R. Candido*, Chiara M. Petrone** and **Riccardo Giusti***

* *Department of Earth Science, University of Florence, Italy.*
** *Department of Earth Sciences, The Natural History Museum, London, U.K.*
° *CNR (National Research Council of Italy) - Institute of Geosciences and Earth Resources, Section of Florence, Italy.*
✉ *Corresponding author, email: enrico.pandeli@unifi.it*

Keywords: *Miocene, Calc-alkaline dykes, Ophiolitic Unit. Northern Apennine, Northern Tyrrhenian Sea, Elba Island.*

ABSTRACT

In this paper we studied in detail magmatic dykes filling fractures in the pillow lavas of the Ophiolitic Unit cropping out in the Monte Capo Stella Promontory (southern part of the Elba Island in the Northern Tyrrhenian Sea). The Elba Island is well known for its Tertiary complex tectonic stack of nappes, Late Miocene intrusion of acidic magmatic bodies and Fe-mineralizations. The phaneritic sub-volcanic rock (Monte Capo Stella dykes, MCSD) shows a porphyritic texture with variable pheno- and xenocrysts content. The main phenocrysts consist of plagioclase, quartz, K-feldspar and biotite. The MSCD, displaying calc-alkaline affinity, have a High-Potassium dacitic composition. Moderate fractionation and negative Eu anomaly characterize the chondrite normalised REE patterns. The mantle-normalised trace element patterns exhibit relatively high content of the most incompatible elements with negative spikes of Ba, Ta, Nb, Sr, P, and Ti. The measured $^{87}Sr/^{86}Sr$ and $^{143}Nd/^{144}Nd$ isotopic ratios are 0.708129 and 0.512209 respectively. In spite of the lack of radiometric data, the MCSD can be related to the acidic to intermediate magmatism that occurred in the interland of the Northern Apennines Chain during Late Miocene-Quaternary times. In particular, the MSCD belong to the intermediate rocks of the Tuscan Magmatic Province and display petrological and geochemical characteristics closely resembling those of a mafic enclave collected in the 6.8 Ma Orano Porphyry (Elba Island) and of some 9-4 Ma High Potassium Calc-Alkaline (HKCA) Capraia Island rocks. Thus, in the context of the Elba Island, the studied dykes represent the magmatic bodies showing the most peculiar HKCA features. The intrusion age of the MCSD can be put in the time interval between the intrusion of the Orano Porphyry in Western Elba (6.8 Ma) and that of the Monte Castello dyke (5.8 Ma) in Eastern Elba, and possibly before the Central Elba Fault (CEF) activity.

This study also refines the deformation history of the Ophiolitic Unit in the Elba Island defining three final brittle deformation stages.

INTRODUCTION

The Elba Island (Northern Tyrrhenian Sea, Figs. 1 and 2) is an intricate and well-known assemblage of Paleozoic to Holocene rocks including Late Miocene plutonic and subvolcanic magmatic bodies, which belong, according to Poli et al. (2003) and Peccerillo (2005), to the Tuscan Magmatic Province (Fig. 1). Its structural framework consists of nappes derived from different paleogeographic domains (Tuscan and Ligurian Domains), piled up together in the Oligocene-Middle Miocene syn-collisional events of the Northern Apennines tectogenesis and then dissected by post-orogenic extensional, low- and high-angle faulting during Middle-Late Miocene to Early Pliocene times (Fig. 2). During the Late Tortonian-Latest Messinian, this structural pile was intruded and thermo-metamorphosed by different, mainly acidic, magmatic bodies like the western-central Elba complex of laccoliths and swarm of dykes and the monzogranitic Monte Capanne and La Serra-Porto Azzurro plutons (Marinelli, 1959; Bortolotti et al., 2001 and references therein; Dini et al., 2002; Fig. 2). The emplacement of the latter bodies produced detachments and deformations in the previously stacked tectonic units too (Trevisan, 1953; Barberi et al., 1969a; 1969b; Pertusati et al., 1993; Bouillin et al., 1994; Bortolotti et al., 2001). In addition, other dykes of variable composition are present in the Ligurian Units in the western (Orano Porphyry in Dini et al., 2002), central (Monte Capo Stella dykes in Bortolotti et al., 2001) and eastern (Monte Castello and Casa Carpini dykes in Conticelli et al., 2001 and Pandeli et al., 2006, respectively) parts of the island. Most of these dykes have been extensively studied and described, but for a few of them (e.g., Monte Capo Stella dykes = MCSD) the available data are still insufficient to completely define their petrological features, the age and the relationships with the intruded host rocks.

In order to contribute to the knowledge of these peculiar magmatic products, we performed a study of the MCSD, which cut the pillow lavas of the Ophiolitic Unit (OU, Monte Strega Unit in the "Carta Geologica d'Italia alla scala 1:50,000, foglio Elba" and the related "Note Illustrative", Principi et al., in progress; see Fig. 3) along the eastern coast of the Monte Capo Stella Promontory, in the southern-central part of the Elba Island (see location in Fig. 2). In our paper we compositionally characterize and describe their setting in order to define their age and relationships with the host ophiolitic basalts and with the other magmatic bodies of the Elba Island.

GEOLOGICAL OUTLINE

The Elba Island (Figs. 1 and 2) is located in the Northern Tyrrhenian Sea, midway between Tuscany (Italy) and Corsica (France). This island plays a key role in the reconstruction of the stratigraphic, tectonic, metamorphic and magmatic evolution of the Northern Tyrrhenian Sea and of the Northern Apennines chain (Barberi et al., 1967; 1969a; 1969b; Pertusati et al., 1993; Bartole, 1995; Bortolotti et al., 2001, and references therein). In particular, the tectonic stack of nappes of the Elba Island is generally considered the innermost outcrop of the Northern Apennines Chain built in the Oligocene-Miocene times. The island is

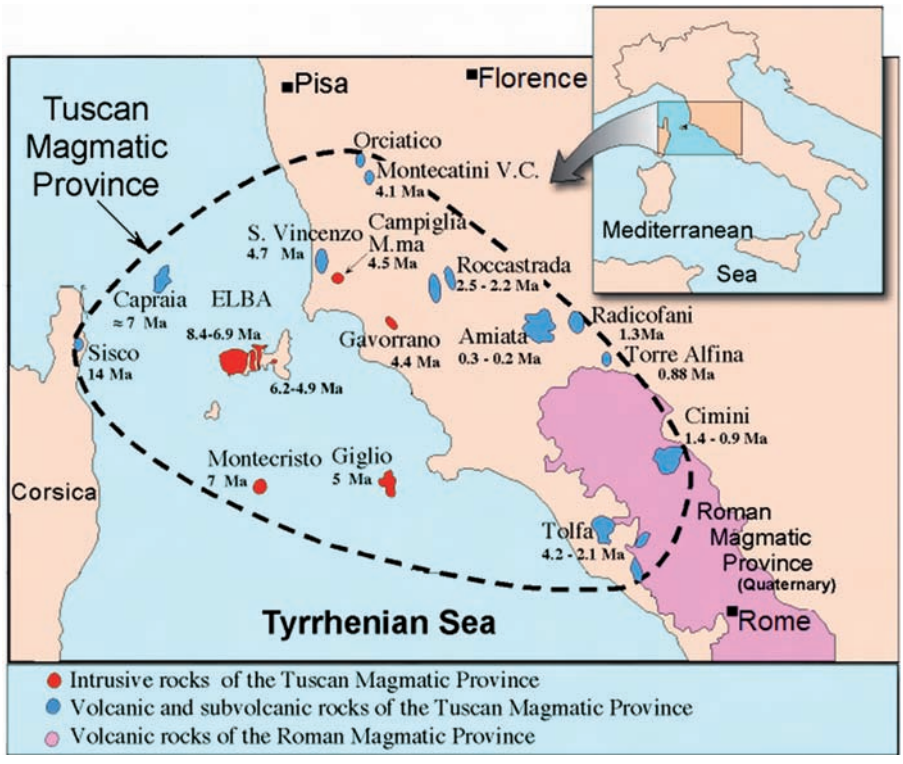

Fig. 1 - Location of the Elba Island and distribution of the Miocene-Quaternary magmatic bodies in the Northern Tyrrhenian Sea and in the inner part of the Northern Apennines (modified from Dini et al., 2006).

also famous for its Fe-ore bodies (e.g., Tanelli et al., 2001) and for the peculiar, and here well exposed, relationships between the intrusion and uplift of the Miocene magmatic bodies and tectonics (Trevisan, 1950; Barberi et al., 1969a; Pertusati et al., 1993; Bouillin et al., 1994; Daniel and Jolivet, 1995; Bortolotti et al., 2001; Maineri et al., 2003; Westerman et al., 2004; Collettini and Holdsworth, 2004; Smith et al., 2013). In fact, during the Middle-Late Miocene time interval, the Elba's tectonic pile experienced post-collisional extensional tectonics (Bortolotti et al., 2001) and was intruded by several Late Miocene magmatic bodies consisting of shallow-level porphyritic laccoliths and dykes of variable acidic composition, two main acidic plutons (the Monte Capanne and the Porto Azzurro, in the western and in the eastern Elba, respectively) and different systems of mafic dykes (Marinelli, 1959; Saupé et al., 1982; Juteau et al., 1984; Ferrara and Tonarini, 1993; Serri et al., 1993; Conticelli et al., 2001; Dini et al., 2002; Rocchi et al., 2002; Maineri et al., 2003; Poli, 2004; Westerman et al., 2004; Pandeli et al., 2006). Moreover, the tectonic stack was mostly remobilized by detachments (e.g., the CEF fault in western-central Elba, Maineri et al., 2003, and the subsequent Zuccale Fault in eastern-central Elba, Bortolotti et al., 2001) during the uplift of the main plutonic bodies.

The Miocene magmatic rocks of the Elba Island (Fig. 1) belong to the complex Tuscan Magmatic Province (TMP), which includes several centres located through Southern Tuscany and the Tuscan Archipelago and is characterised by a large variety of intrusive and effusive rock types closely associated in space and time; these magmatic rocks show an evident younging towards east throughout the chain (Marinelli, 1961; Peccerillo et al., 1987; Serri et al., 1993; Dini et al., 2002; Peccerillo and Donati, 2003; Peccerillo, 2005).

Particularly during the Tortonian-Early Pliocene times, mafic sub-volcanic and volcanic rocks (e.g., the 9-4 Ma High-K calc-alkaline and shoshonitic lavas of the Capraia Island, the 4.1 Ma Orciatico and 4.2 Ma Montecatini Val di Cecina lamproites, the 6.8 Ma Orano Porphyry in western Elba, the 5.8 Ma Mt. Castello dyke in the eastern Elba) and anatectic, locally hybrid, sub-volcanic and plutonic rocks (e.g., the 6.9 Ma Monte Capanne and the 5.9 Ma Porto Azzurro plutons in western and eastern Elba Island respectively, the 8-7.4 Ma Christmas-tree laccolitic and dyke complex of central Elba Island, the 4.7-3.2 Ma San Vincenzo rhyolites and the 4.5 Ma Campiglia pluton along the Tuscan coast, the 7 Ma Montecristo Isle pluton, the 5 Ma Giglio Isle pluton and the 4.4 Ma Gavorrano pluton) were emplaced in this innermost part of the Northern Apennines chain (e.g., Peccerillo et al., 1988; Serri et al., 1993; Conticelli et al., 2001; Dini et al., 2002; 2006; Figs. 1 and 2).

According to Poli (2004), all these magmatic products can be subdivided in three main groups of rocks: 1) mafic rocks, dykes and mafic-intermediate enclaves, compositionally very complex, ranging from calc-alkaline and shoshonitic to potassic and ultra-potassic, 2) intermediate-acid rocks, generally showing petrographic and geochemical evidence of magma interaction processes such as, for instance, the occurrence of mafic microgranular enclaves (MME), and 3) silicic rocks which exhibit typical characteristics of anatectic melts, originated in the crust and displaying no mixing evidence. The silicic rocks of the Tolfa-Manziana-Cerite area (NW of Rome) and a mafic dyke from Sisco (Corsica) are also traditionally included in the TMP (Poli et al., 2003).

More recently, Conticelli et al. (2007; 2010) and Avanzinelli et al. (2008; 2009) proposed a new subdivision of the Tuscan Magmatic Province, distinguishing: a) the ultrapotassic orogenic Corsican Magmatic Province (lamproitic Sisco dykes and shoshonitic and High-K calc-alkaline volcanites of Capraia Island), b) the mafic volcanic and sub-volcanic rocks (Tuscan Magmatic Province) and c) the acidic anatectic magmatic intrusive and effusive rocks (Tuscan Anatectic Province) of Tuscany.

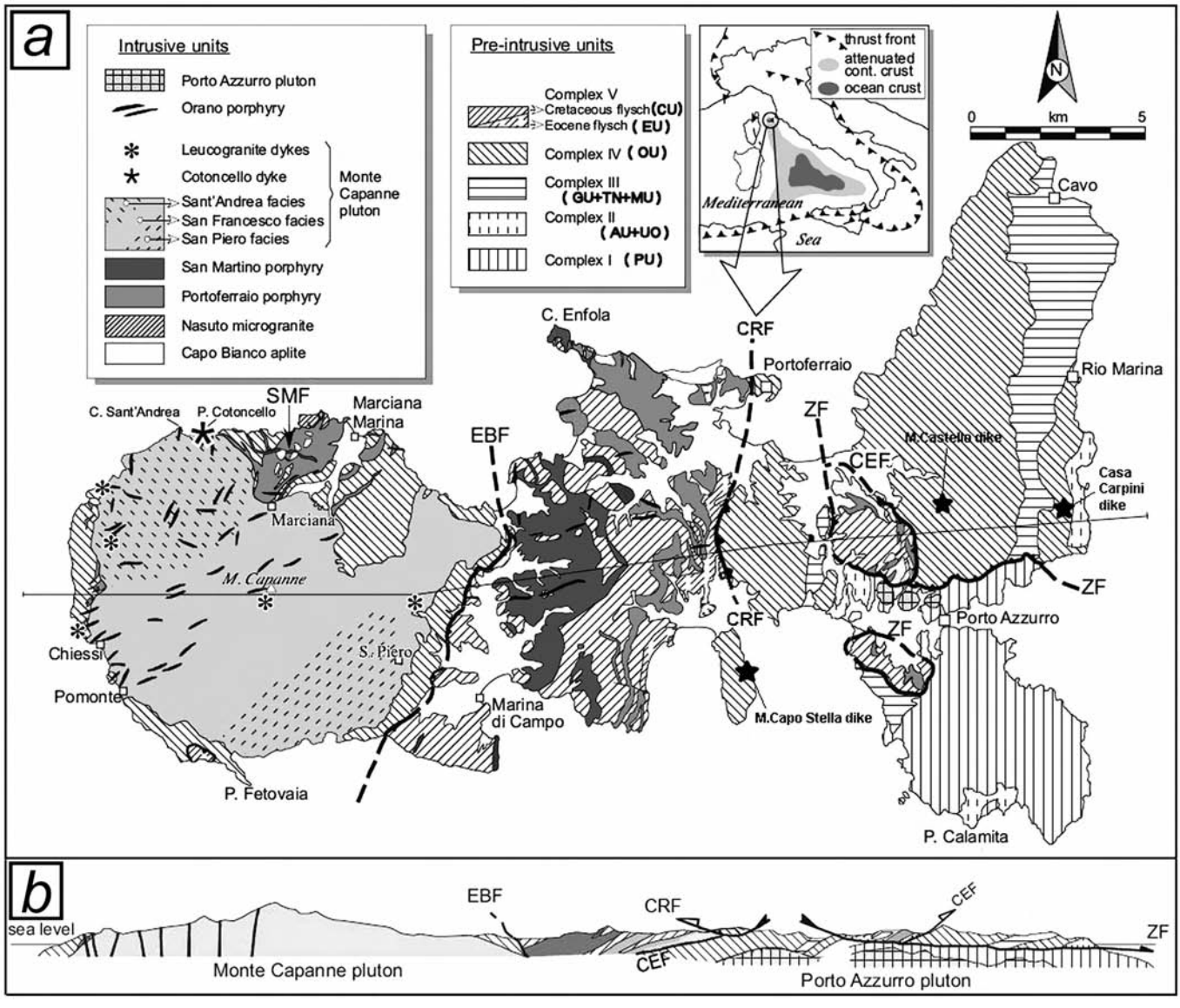

Fig. 2 - Geological map (a) and section (b) of the Elba Island with reported the different magmatic bodies (modified from Westerman et al., 2003). EBF = Eastern Border Fault, CEF = Central Elba Fault, ZF = Zuccale Fault, CRF = Colle Reciso Fault. The correspondence of the five Trevisan's Complexes with the Bortolotti's Units is reported in the legend of the pre-intrusive Units: PU = Porto Azzurro Unit; UO = Ortano Unit; AU = Acquadolce Unit; MU = Monticiano-Roccastrada Unit; TN = Tuscan Nappe; GU = Gràssera Unit; OU = Ophiolitic Unit; EU = Paleogene Flysch Unit; CU = Cretaceous Flysch Unit.

According to several authors (e.g., Boccaletti and Guazzone, 1972; Maliverno and Ryan, 1986; Patacca and Scandone, 1989; Serri et al., 1993; Jolivet et al., 1998; Conticelli et al., 2010; Balestrieri et al., 2011), this magmatic activity was linked to orogenic processes related to crustal subduction, back-arc extensional crustal thinning and rising of the asthenosphere coupled with the eastward rollback and retreat of the west-dipping Adriatic slab and to the eastward migration of the orogenic front.

The 1:10.000 scale geological mapping for the "Carta Geologica d'Italia" 1:50.000 scale (in progress, ISPRA-CARG Project) of Elba Island partially published at 1:14.000 scale by Babbini et al. (2001), in Bortolotti et al. (2001), revealed a more complex geological framework when compared to the Trevisan's classical one (Trevisan, 1950; Barberi et al., 1969a), which was based only on five tectonic "Complexes" (see Figs. 2 and 3). In the Bortolotti's tectonic model (Fig. 3), nine units were distinguished and related respectively to the Tuscan (i.e. the metamorphic Porto Azzurro-PU, Ortano-UO, Monticiano-Roccastrada-MU Units and the unmetamorphic Tuscan Nappe-TN Unit), and Ligurian-Piedmontese (i.e. the unmetamorphic Ophiolitic Unit-OU, Paleogene Flysch Unit-EU and Cretaceous Flysch Unit-CU (the last two, Lacona Unit and Ripanera Unit respectively, in the "Carta Geologica d'Italia alla scala 1:50,000, foglio Elba" and the related "Note Illustrative", Principi et al., in progress) and the metamorphic Acquadolce Unit-AU and Gràssera Unit-GU paleogeographic domains (see the schematic sketch in Fig. 3). The tectonic interposition of the metamorphic Ligurian-Piedmontese Units at different levels in the stack of nappes is a peculiar feature respect to the other parts of the Northern Apennines chain. In general, the tectonic pile of the upper eight imbricated main structural units, separated by west-dipping, low angle tectonic surfaces (thrusts and detachments), lays onto the lowermost Porto Azzurro Unit by the Zuccale low-angle detachment fault, characterized by a decametric cataclastic horizon (Figs. 2b and 3). This peculiar attitude is related to the complex evolution of the Elba Island.

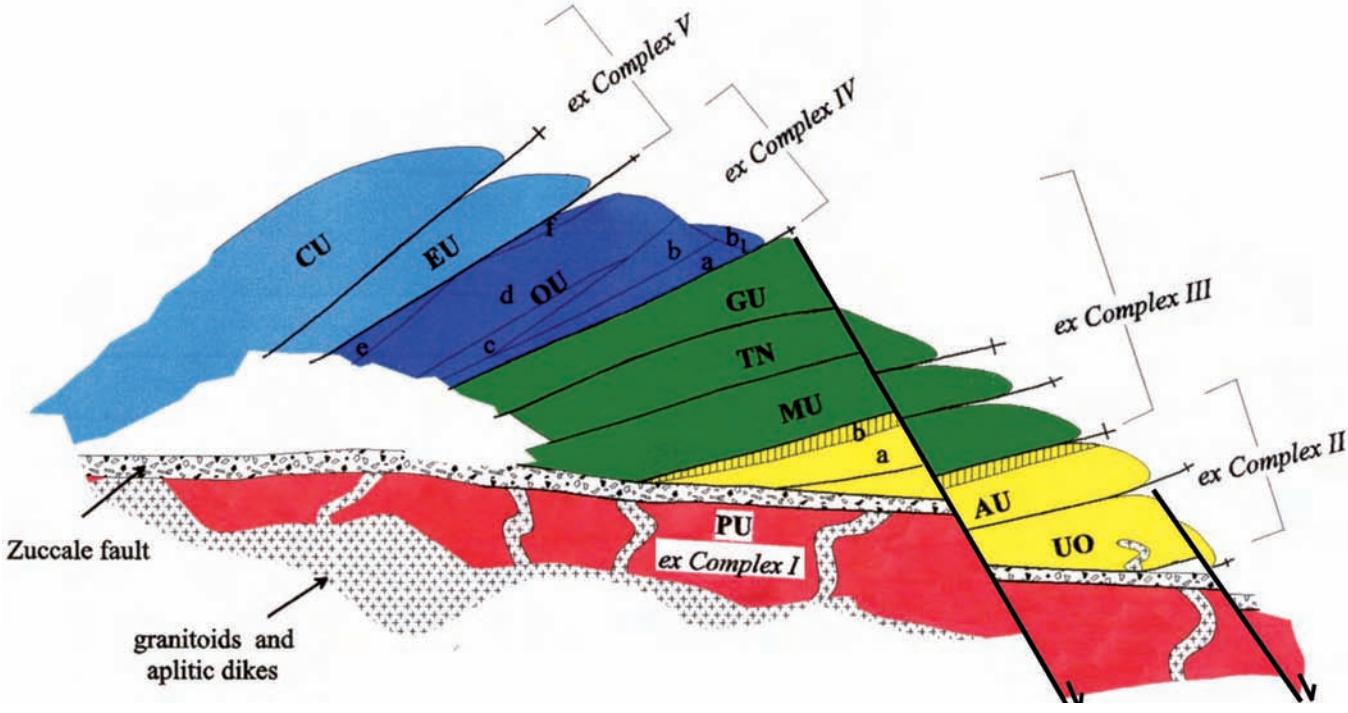

Fig. 3 - The central and eastern Elba tectonic pile, according to Bortolotti et al. (2001), and correspondence with the Trevisan's complexes. PU = Porto Azzurro Unit; UO = Ortano Unit; AU = Acquadolce Unit (a: Porticciolo Subunit; b: Santa Filomena Subunit); MU = Monticiano-Roccastrada Unit; TN = Tuscan Nappe; GU = Gràssera Unit; OU = Ophiolitic Unit (a: Acquaviva Subunit; b: Monte Serra Subunit; b1: Capo Vita Subunit; c: Sassi Turchini Subunit; d: Volterraio Subunit; e: Magazzini Subunit; f: Bagnaia Subunit); EU = Paleogene Flysch Unit; CU = Cretaceous Flysch Unit.

Moreover, Garfagnoli et al. (2005) and Smith et al. (2013) suggested that the uplift of the Porto Azzurro pluton also arched and reactivated the Zuccale Fault itself producing its present dome shape and the eastward and westward (see the Colle Reciso Fault in Fig. 2, as defined by Bortolotti et al., 2001) final slidings of the embricated stack of units. Pre- and post Zuccale high-angle faulting events are also recognizable: a) a mostly NE-SW trending and, locally, a NW-SE transfer-type fault systems predating the Zuccale Fault, can be identified in the Ophiolitic Unit, north of Porto Azzurro (Babbini et al., 2001; Bortolotti et al., 2001; Garfagnoli et al., 2005), b) a NW-SE/NE- SW (in the Calamita Promontory) and N-S (from Porto Azzurro to Cavo) directed block faulting, cutting the whole tectonic pile and detachments, post-date the Zuccale fault). The N-S-trending faults are locally sealed by hematite-rich mineralization dated about 5 Ma by Lippolt et al. (1995).

GEOLOGICAL DATA FROM MONTE CAPO STELLA PROMONTORY

This promontory is mostly made up by Ophiolitic Unit lithotypes and, subordinately, by Quaternary clastic rocks (Fig. 4). These latter are represented by yellowish, more or less cemented, aeolian sands (often characterized by cross-stratification and local micro-conglomeratic horizons) cropping out along the western and southeastern coasts of the promontory. In addition, Holocene sandy and gravelly beach sediments and eluvial and colluvial detrital covers are present, particularly in the northern part of the studied area. The Ophiolitic Unit is mainly represented by Middle-Late Jurassic basaltic pillow lava (up to 1 m in size), grey-greenish to dark green in color, which, sometimes, shows variolitic textures on the external parts. Pillow breccias and ialoclastites are locally associated to these volcanic rocks. Basalts display a sedimentary cover made by a few slices of Early Cretaceous calcareous-marly (Nisportino Fm.) and calcareous-cherty (Calpionella Limestones Fm.) rocks, which tectonically overlie the pillow lavas through W-NW - dipping low-angle faults (Fig. 4).

The studied dykes are exposed along the eastern coast of the Capo Stella Promontory (NNE of the Casa Mazzari locality, see location in Fig. 2 and magnification in Fig. 4).

These decimetric up to 130 cm-thick, light grey to brownish porphyritic magmatic bodies fill a high to medium angle fracture network, generally characterized by a NW-SE strike and a SW dip, in the Jurassic pillow lavas, pillow breccias and ialoclastites of the Ligurian Ophiolitic Unit (Figs. 4, 5a, b and 6a).

The same NW-SE directed fracture network is locally sealed by quartz ± epidote ± chlorite veins that sometimes cuts the pillow basalt-dyke contact. At places, the final filling of the veins is represented by chlorite. Some centimetric to decimetric quartz veins, inside the pillow lavas, abruptly end at the contact with the dykes and can be likely related to the Ligurian Jurassic oceanic hydrothermalism (Fig. 7).

A medium- to low-angle, top-to-the-east faulting (reverse at the outcrop scale) displaced the dykes. This faulting event is characterized by a N-S to ENE-WSW strike, western dip and decimetric to 1.5 meter of throw (see Figs. 6a and 8a b). Finally a medium- to high- angle, NE-SW and NW-SE directed fracture network cuts all the previous structures (Fig. 6b). These latter fractures have often represented the pathway for the circulation of Fe oxides/hydroxides-rich fluids (Fig. 8c).

The contact between the dykes and the host rock is sharp (Figs. 5b and 8a, b, c) and is locally underlined by Fe-oxide/hydroxide mineralization. K-feldspar phenocrysts, up to

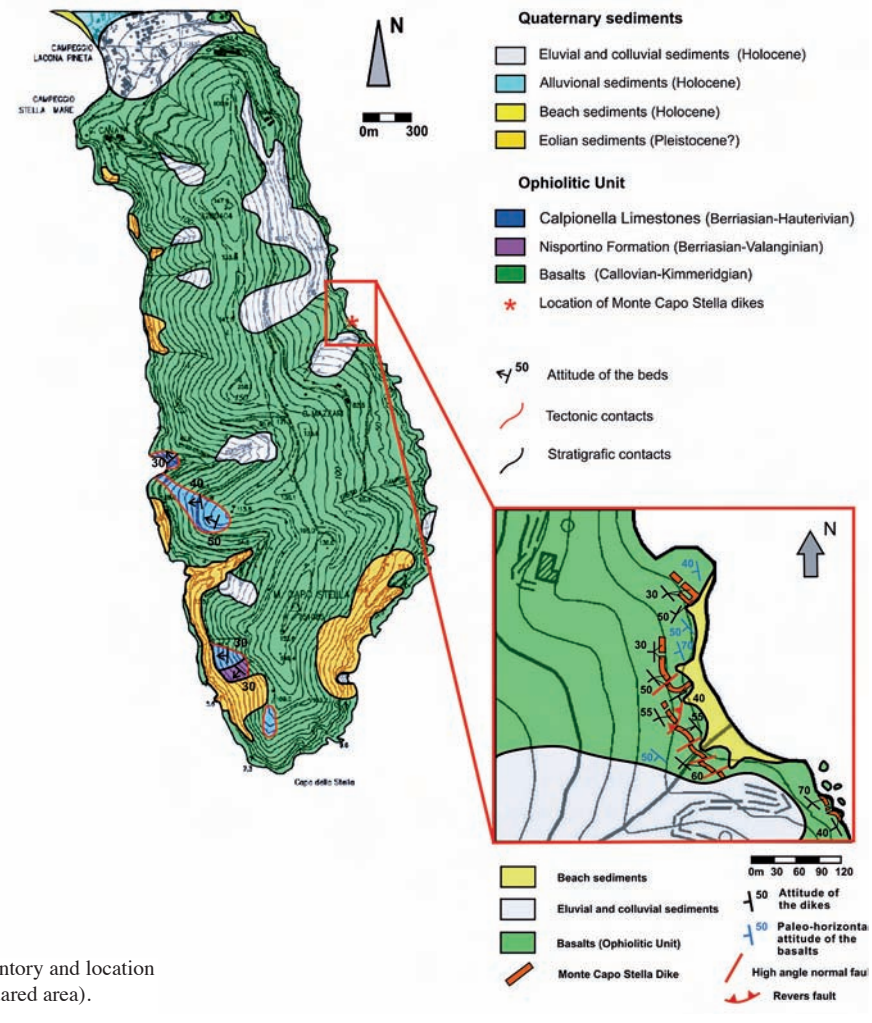

Fig. 4 - Geological map of the Monte Capo Stella Promontory and location of the Monte Capo Stella dykes (see magnification of squared area).

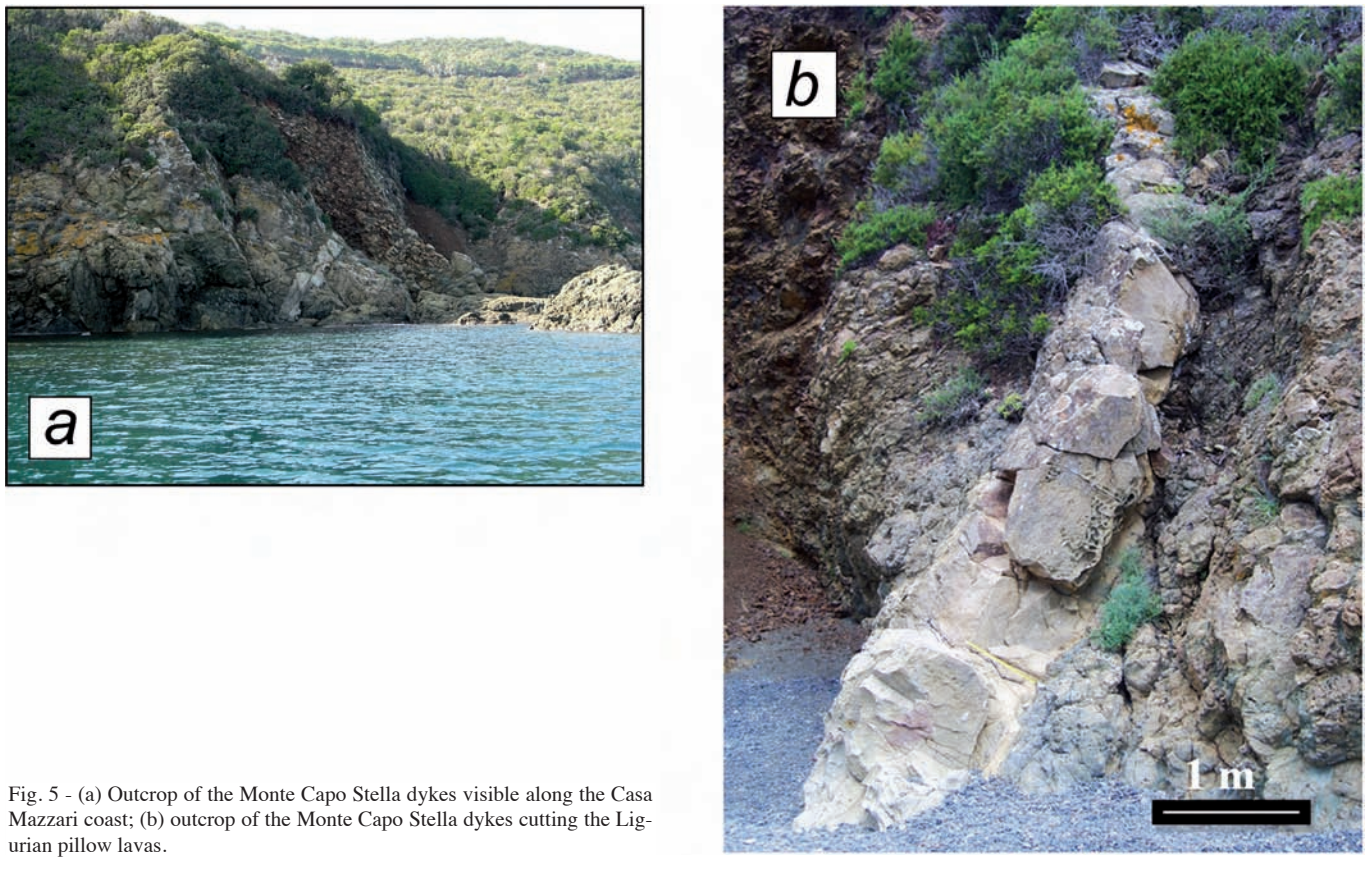

Fig. 5 - (a) Outcrop of the Monte Capo Stella dykes visible along the Casa Mazzari coast; (b) outcrop of the Monte Capo Stella dykes cutting the Ligurian pillow lavas.

decimetric in size, are sometimes recognizable in the fine-grained chilled margins of the dykes (Fig. 8b). Moreover, in the peripheral part of the dyke a weak isorientation of biotite and plagioclase, parallel to the dyke boundaries is present; this lineation is likely related to magmatic flow. No tectonic ductile deformations or recrystallizations are evident in the texture of both MCSD and host pillow lavas both at the meso- and micro-scale.

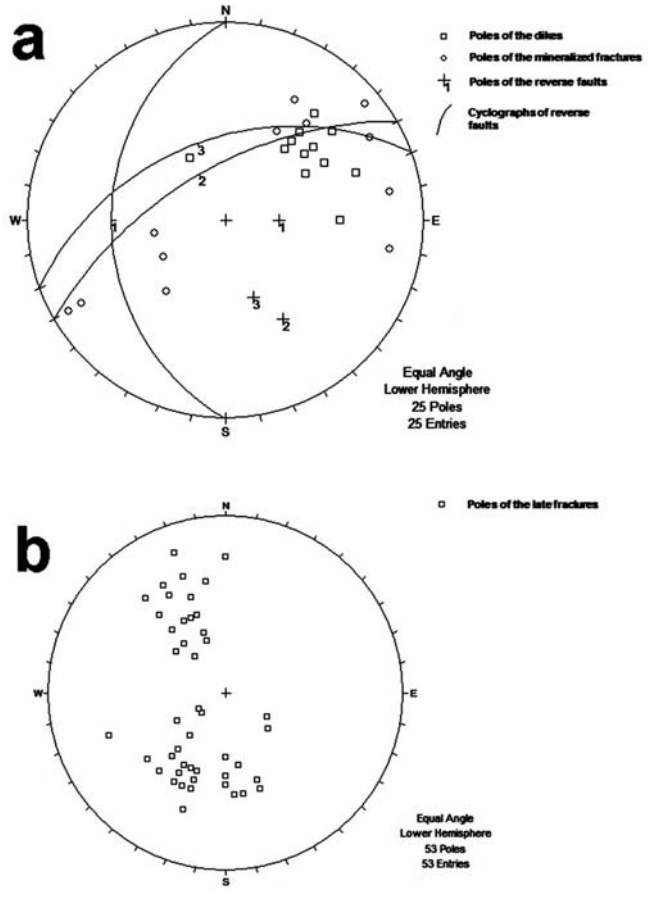

Fig. 6 - (a) Poles of the Monte Capo Stella dykes and fractures filled by hydrothermal mineralizations; the cyclographic curves are related to the reverse faults; (b) poles of the later fractures.

SAMPLING AND RESULTS

Several rock samples, for petrographic and geochemical analyses (see below), were collected from the dykes in the Casa Mazzari area. Mineral and whole rock (major, trace elements and Sr and Nd isotope) compositions for representative dyke samples are reported in Tables 1 and 2. Analytical procedures used for minerals and rock samples are described in the Appendix.

Petrography and Mineral Chemistry

The phaneritic sub-volcanic rock forming the dykes displays a porphyritic texture with variable pheno- and xenocryst content. The mineralogy of the dykes consists of twinned subhedral to euhedral, zoned plagioclase (Pl), subhedral to anhedral quartz (often characterized by embayment), subordinate euhedral to subhedral K-feldspar (Kfs) phenocrysts, up to 7 mm in size (Fig. 9) and biotite. Rare greenish to brownish calcic amphibole is present as microphenocryst. Notably, K-feldspar is also present as very large phenocrysts, 3.5 x 1.5 cm in size on the average (max 10 x 2 cm). A common characteristic of the Capo Stella main mineral phases, is the presence of a sub-millimetric resorbed rim (Fig. 9c). Fe and Ti-oxides, apatite, zircon and epidote are ubiquitous accessory minerals. The microcrystalline groundmass is composed of xenomorphic quartz and K-feldspar, plagioclase microliths, biotite and minor amphibole (Fig. 9b). In the peripheral parts of the dyke, the groundmass is locally characterized by the presence of sub-millimetric irregular, spherical to ellipsoidal spots, texturally resembling a perlite, but not completely resolvable under the optical microscope (Fig. 9a). Opaque minerals, sericite, chlorite, and clay mineral films underline these spots. The contact of the dyke with the surrounding pillow lavas is sharp also at the microscopic scale and the outermost part of the dyke sometimes shows a variation in texture from microcrystalline (with plagioclase and generally chloritized biotite crystals) to aphanitic.

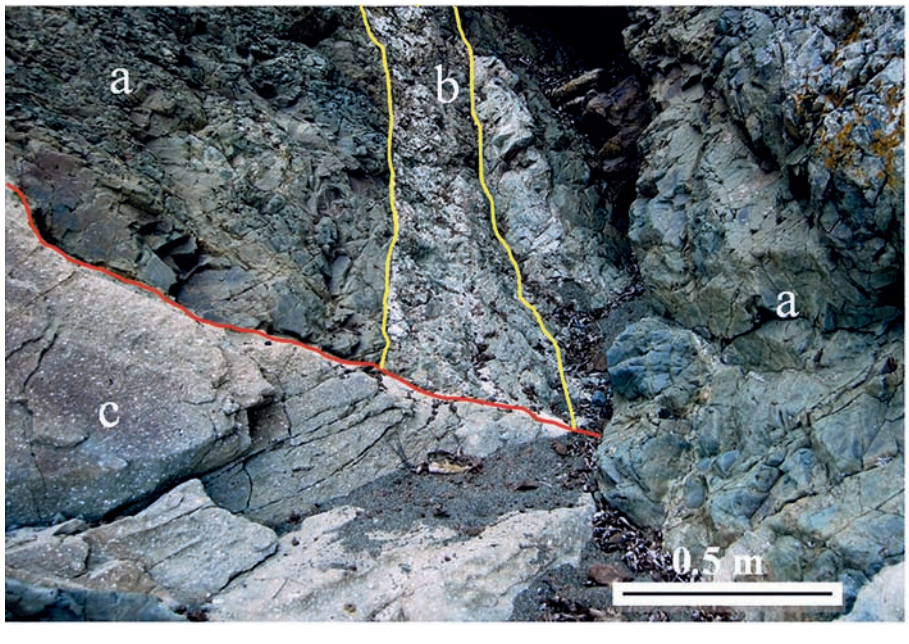

Fig. 7 - Decimetric quartz veins (b) within the pillow lavas (a) cut by the Monte Capo Stella dykes (c) veins.

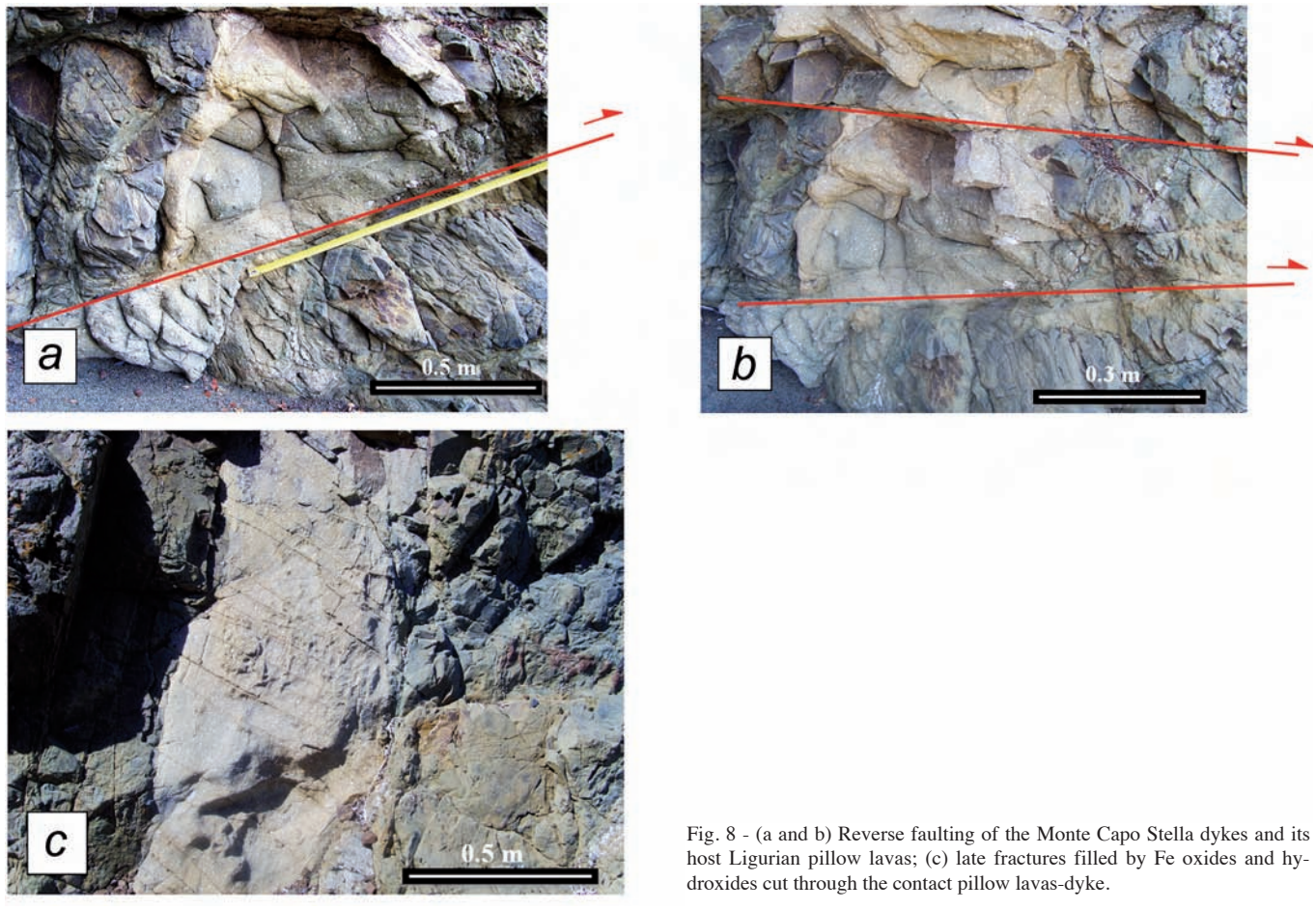

Fig. 8 - (a and b) Reverse faulting of the Monte Capo Stella dykes and its host Ligurian pillow lavas; (c) late fractures filled by Fe oxides and hydroxides cut through the contact pillow lavas-dyke.

Table 1 displays representative electron microprobe analyses of the main mineral phases observed in the Monte Capo Stella dykes. In the studied rocks, plagioclase (Fig. 9b, d) represents by far the most abundant mineral. It displays a wide range of textures (clear, sieved, patchy, turbid) and composition (core composition in the range Ab_{34-99}, $An_{0.4-66}$, $Or_{0.3-4.4}$); zoning is slight, normal or reverse; the turbid and resorbed crystals, showing a very Ab-rich core ($Ab_{85-99\%}$), are considered of possible xenocrystic origin. High compositional variability is displayed also by the Pl rim (Ab_{24-87}, An_{12-75}, $Or_{0.6-21}$) and by the small crystals contained in the groundmass (Ab_{31-89}, An_{10-68}, $Or_{0.6-8}$). The presence of some groundmass crystals showing Ab content higher than coexisting phenocrysts testify disequilibrium between crystals and liquid. Locally, epidote alteration and pseudomorphic substitution of the plagioclase phenocrysts are evident.

K-feldspar, that generally shows the optical features of sanidine, displays core composition variable in the range $Or_{79-94\%}$ whereas the Or content in the rim is variable between 51 and 85%; large Or-rich crystals (Or content in the core exceeding 93%), often characterised by inclusions of plagioclase and biotite, are abundant; a xenocrystic origin is hypothesised also for these crystals. Sometimes an epitaxial nucleation of K-feldspar mantles the plagioclase phenocrysts showing a typical "anti-Rapakivi" texture (cfr. Type E mantle feldspar in Hibbard, 1981). Biotite is partly or completely transformed in chlorite. According to Leake et al. (1997), the Capo Stella amphibole can be classified as edenite.

GEOCHEMISTRY

Major and trace element composition of representative Monte Capo Stella rock samples, collected in two different outcrops along the beach, is reported in Table 2 together with the Sr and Nd isotopic ratios of one rock sample. The reported compositions correspond to the inner portions of the dykes.

According to the alkali-silica classification diagram (Le Bas et al., 1986), the two analysed rock samples can be classified as dacites (Fig. 10a) belonging to the High-K calc-alkaline series (Fig. 10b). Samples collected in the inner part of the dykes, only partially interested by alteration (see petrography and LOI values), display an overall similar composition.

For comparison, in order to show the wide compositional variability of some mafic-intermediate Tuscan magmatic products, in Fig. 10a, are reported, also, the composition of other Elba dykes (Dini et al., 2002; Pandeli et al., 2006), the composition of the other intermediate Tuscan calc-alkaline rocks (Capraia Island; Prosperini, 1993; Conticelli et al., 2009) and the composition of the microgranular mafic enclave (MME) PP-333 collected in the Orano Porphyry (Dini et al., 2002); this latter plays an important role as, following Poli (1992), the enclaves present in the Orano Porphyry may be considered as blobs of mafic-intermediate melts intruded into and mingled with the cooler acidic host magma.

Chondrite normalised (McDonough and Sun, 1995) REE patterns (Fig. 11a, b), of the Monte Capo Stella rock samples, are similar; they are characterised by moderate

Table 1 - Representative chemical analyses of the main mineral phases.

	plagioclase																											
sample	STE 1	STE 1	STE 1	STE 3		STE 3		STE 3					STE 3		STE 3	STE 3		STE 3		STE 3		STE 3	STE 3	STE 3	STE 3	STE 3	STE 3	STE 3	STE 3
	pheno rim	pheno rim	gdm	pheno core	pheno rim	pheno core	pheno rim	pheno core	outer core	outer core	inner rim	pheno rim	pheno core	pheno rim	pheno core	pheno core	pheno rim	pheno core	pheno rim	pheno core	pheno rim	gdm	gdm	gdm	gdm	gdm	gdm	enclave	enclave
SiO_2	59.2	62.1	64.8	64.0	65.7	63.8	64.2	60.6	62.9	59.8	60.7	63.7	61.0	56.9	67.3	62.0	58.0	51.2	50.2	60.5	60.0	51.5	51.4	51.4	52.8	67.1	64.3	69.7	68.3
Al_2O_3	25.7	24.3	22.7	22.8	22.0	23.1	22.7	25.1	24.0	25.7	24.5	23.6	24.6	27.2	19.9	23.7	26.2	30.1	31.3	24.5	24.9	30.2	30.3	30.4	29.2	21.3	22.5	19.4	20.1
Fe_2O_3	0.07	0.04	0.09	0.04	0.05	0.06	0.02	0.01	0.02	0.06	0.06	0.15	0.04	0.10	1.42	0.02	0.07	0.21	0.23	0.04	0.05	0.35	0.38	0.36	0.40	0.21	0.34	0.27	0.30
CaO	8.1	5.9	4.0	3.6	3.2	4.3	4.0	7.0	5.1	7.5	6.3	4.8	6.7	9.8	6.1	5.4	8.2	13.7	14.5	6.6	7.0	13.5	13.6	13.6	12.3	2.2	3.8	0.09	0.83
Na_2O	6.4	8.1	9.1	9.4	9.5	9.3	9.0	7.5	8.6	6.8	7.5	8.9	7.2	5.6	6.1	8.7	6.6	3.7	3.1	7.2	6.9	3.6	3.4	3.4	4.3	10.2	9.3	11.7	11.1
K_2O	0.6	0.13	0.11	0.08	0.10	0.11	0.39	0.11	0.14	0.56	0.51	0.16	0.73	0.33	0.32	0.11	0.53	0.19	0.19	0.77	0.69	0.21	0.22	0.17	0.26	0.18	0.13	0.05	0.07
Sum	100.1	100.5	100.8	100.0	100.7	100.8	100.3	100.3	100.8	100.4	99.7	101.3	100.3	100.1	101.5	100.0	99.6	99.2	99.7	99.7	99.5	99.6	99.5	99.5	99.4	101.1	100.4	101.2	100.8
An	56.8	70.8	79.9	82.2	83.7	79.3	78.7	65.6	74.5	60.1	66.1	76.4	63.3	49.7	63.0	74.1	57.4	32.5	27.4	63.4	61.5	32.2	30.7	31.0	38.3	88.5	81.0	99.3	95.7
Ab	39.7	28.5	19.5	17.3	15.7	20.1	19.1	33.8	24.7	36.7	30.9	22.7	32.5	48.3	34.8	25.3	39.5	66.4	71.4	32.1	34.5	66.6	67.9	68.0	60.2	10.5	18.2	0.4	3.9
Or	3.5	0.73	0.63	0.48	0.58	0.59	2.2	0.60	0.83	3.2	3.0	0.88	4.2	1.9	2.2	0.60	3.1	1.1	1.1	4.4	4.0	1.2	1.3	1.0	1.5	1.0	0.76	0.30	0.40

	K-feldspar														biotite			chlorite								
	STE 1			STE 1	STE 1	STE 1	STE 1	STE 3	STE 3	STE 3	STE 3	STE 3	STE 3		STE 3	STE 3		STE 1	STE 1	STE 3	STE 3	STE 3	STE 3	STE 3	STE 3
	pheno core	outer core	inner rim	pheno rim	pheno core	pheno core	gdm	gdm	pheno core	pheno core	pheno core	pheno rim	pheno core	gdm	pheno core	pheno core										
SiO_2	64.4	64.9	64.5	65.3	65.2	65.3	65.1	66.7	75.6	89.5	74.4	57.9	64.4	81.2	SiO_2	36.8	36.2	SiO_2	34.70	35.71	31.03	33.50	32.50	33.12	28.03	28.18
Al_2O_3	18.5	19.0	18.7	18.6	18.2	17.5	18.6	17.5	13.2	5.9	11.5	18.0	18.2	8.7	TiO2	3.9	3.9	Al_2O_3	17.27	17.08	18.16	17.02	16.67	16.48	19.90	19.36
Fe_2O_3	0.04	0.08	0.03	0.09	0.01	0.07	0.12	0.13	0.23	0.10	1.6	3.6	0.03	1.03	Al_2O_3	14.6	14.5	FeO	15.48	14.83	16.05	15.92	17.28	17.80	19.67	19.78
CaO	0.02	0.16	0.15	0.19	0.01	0.23	0.67	0.21	0.49	0.30	0.21	1.2	0.05	0.06	FeO	18.5	18.7	MnO	0.20	0.21	0.26	0.23	0.25	0.27	0.30	0.27
Na_2O	0.71	1.48	1.61	2.12	0.60	0.63	2.99	0.38	1.21	0.44	0.34	1.1	0.59	0.20	MnO	0.27	0.23	MgO	17.72	17.63	19.67	17.36	19.68	18.35	18.03	17.52
K_2O	16.0	14.6	15.1	12.9	15.6	15.0	11.6	14.3	8.6	4.0	7.5	8.2	14.0	6.3	MgO	10.5	10.7	CaO	1.06	1.46	0.56	0.70	0.52	0.80	0.08	0.14
															CaO	0.15	0.09	Na_2O	0.22	0.40	0.43	0.33	0.23	0.26	0.00	0.03
Sum	99.6	100.2	100.0	99.1	99.6	98.8	99.1	99.2	99.3	100.3	95.5	90.1	97.3	97.5	Na_2O	0.17	0.19	K_2O	0.74	0.54	0.19	1.71	0.04	0.05	0.10	0.43
															K_2O	8.2	8.8	Cr_2O_3	0.43	0.40	0.10	0.00	0.84	0.70	0.04	0.04
An	6.3	13.2	13.9	19.8	5.5	5.9	27.3	3.9	17.0	13.7	6.3	15.2	6.0	4.7												
Ab	0.10	0.79	0.71	0.98	0.05	1.2	3.4	1.2	3.8	5.1	2.2	9.3	0.30	0.74	Sum	93.1	93.3	Sum	87.40	87.87	86.36	86.96	87.18	87.13	86.18	85.92
Or	93.6	86.0	85.4	79.2	94.4	92.9	69.4	95.0	79.1	81.1	91.5	75.5	93.7	94.6	Mg no.	0.50	0.50	Mg no.	67.11	67.94	68.60	66.02	66.98	64.74	62.03	61.22

	amphibole																	epidote							oxide
	STE 1	STE 3	STE 3	STE 3	STE 3	STE 3	STE 3	STE 3	STE 3	STE 3	STE 3	STE 3	STE 3	STE 3	STE 3	STE 3	STE 3	STE 3	STE 3	STE 3	STE 3	STE 3	STE 3		STE 3
	gdm	core	core	core	core	core	core	rim	micro core	gdm	micro core	gdm	micro core	micro core	core	rim	gdm									
SiO_2	46.7	44.0	43.4	44.7	43.4	45.1	45.3	44.5	44.4	44.6	46.6	43.8	47.6	44.5	45.2	44.6	44.6	SiO_2	38.6	38.2	39.2	39.0	38.2	38.3	SiO_2	30.1
TiO2	2.4	2.7	2.9	3.0	3.3	2.9	2.7	3.1	2.7	3.1	2.9	2.8	1.7	3.1	2.5	2.7	2.8	TiO2	0.16	0.03	0.13	0.18	0.17	0.15	TiO2	4.4
Al_2O_3	11.0	10.2	11.8	10.4	10.5	11.0	10.8	11.3	11.2	11.1	10.8	10.5	7.8	10.0	10.6	10.9	10.7	Al_2O_3	26.6	25.4	23.9	24.8	24.6	24.9	Al_2O_3	0.19
FeO	12.0	14.0	10.6	10.8	10.9	8.8	10.5	9.8	9.7	9.4	9.4	12.8	12.6	11.3	11.2	11.1	11.8	FeO	8.0	9.5	10.4	9.7	10.0	10.0	FeO	0.03
MnO	0.18	0.15	0.13	0.16	0.15	0.11	0.18	0.14	0.11	0.12	0.14	0.17	0.22	0.13	0.16	0.13	0.21	MnO	0.23	0.23	0.11	0.10	0.15	0.14	MnO	0.01
MgO	11.6	12.6	14.5	14.1	14.2	15.5	14.7	14.9	14.9	15.2	14.8	12.4	14.6	14.2	14.9	13.9	13.3	MgO	0.04	0.07	0.16	0.61	0.05	0.03	MgO	27.9
CaO	10.8	10.6	11.0	11.4	11.0	11.5	11.1	11.2	11.1	11.1	11.2	10.8	10.6	11.1	10.5	11.2	10.8	CaO	23.3	23.3	23.1	23.1	23.2	23.4	Cr_2O_3	1.1
Na_2O	1.8	1.7	1.9	1.8	1.9	1.8	1.8	1.8	1.8	1.8	2.0	1.9	1.4	1.8	1.9	1.8	1.8								NiO	0.27
K_2O	0.83	0.77	0.75	0.86	0.75	0.72	0.65	0.74	0.73	0.69	0.70	0.80	0.51	0.74	0.62	0.73	0.76									
Sum	97.8	97.0	96.9	97.7	96.6	97.8	97.9	97.7	97.0	97.5	99.0	96.5	97.5	97.1	97.9	97.3	97.1	Sum	96.9	96.8	96.9	97.5	96.4	97.0	Sum	95.6
Mg no.	0.63	0.61	0.71	0.70	0.70	0.76	0.71	0.73	0.73	0.74	0.73	0.63	0.67	0.69	0.70	0.69	0.66									

pheno = phenocryst; microph = microcrystal; gdm = crystal in groundmass; An = anorthite; Ab = albite; Or = orthoclase.

Table 2 - Representative major (%) and trace (ppm) element and isotopic (Sr and Nd) composition of the Monte Capo Stella dykes.

sample	STE 1	STE 3
SiO_2	62.38	62.77
TiO_2	0.67	0.66
Al_2O_3	15.92	15.25
Fe_2O_3	5.07	5.03
MnO	0.07	0.07
MgO	3.68	3.79
CaO	2.42	2.42
Na_2O	3.15	3.03
K_2O	3.26	3.08
P_2O_5	0.17	0.17
LOI	3.73	3.32
Sum	100.5	99.58
Sc	14	14
V	89	91
Cr	190	190
Co	14	14
Ni	30	20
Rb	69	65
Sr	320	316
Y	17.6	18.1
Zr	148	143
Nb	12.8	10.5
Cs	2.7	2.6
Ba	418	425
La	25.8	29.2
Ce	50.0	55.9
Pr	6.21	6.79
Nd	24.6	25.7
Sm	4.83	5.19
Eu	1.15	1.18
Gd	4.14	4.14
Tb	0.63	0.63
Dy	3.41	3.45
Ho	0.65	0.66
Er	1.80	1.82
Tm	0.28	0.26
Yb	1.87	1.75
Lu	0.28	0.26
Hf	4.0	3.8
Ta	0.98	1.03
Pb	22	18
Th	11.5	12.6
U	6.02	6.17
$^{87}Sr/^{86}Sr$		0.708129 ± 0.000007
$^{143}Nd/^{144}Nd$		0.512209± 0.000008

LREE/HREE fractionation with $(La/Yb)_N$ = 9.4, 11.3 and negative Eu anomaly. The Orano Porphyry (Dini et al., 2002) displays more fractionated REE patterns at higher absolute LREE-MREE abundances (Fig. 11a). In contrast, the Monte Capo Stella REE patterns closely resemble that of the microgranular mafic enclave PP-333, whereas the Capraia calc-alkaline rocks (Prosperini, 1993; Conticelli et al., 2009) generally display subparallel REE patterns at higher abundances with respect to the Monte Capo Stella dykes.

The mantle-normalised (Sun and McDonough, 1989) trace element patterns (Fig. 12a, b) for the rock samples from the inner portion of the dykes are virtually indistinguishable and show relatively high content of the most incompatible elements, with negative spikes of Ba, Ta, Nb, Sr, P, and Ti; they fall at the lower limit of the Orano Porphyry range (Dini et al. 2002; Fig. 12a) and display lower content of several elements (e.g., Cs, Rb, Ba, Sr) than Capraia HKCA rocks (Prosperini, 1993; Conticelli et al., 2009; Fig. 12b). The trace element patterns of the Monte Capo Stella dykes display good similarities with the mafic enclave PP-333 pattern (Dini et al., 2002) except for the most incompatible elements, Cs and Rb, which are lower in the Monte Capo Stella dykes and comparable to HKCA rocks from Aeolian Islands (e.g., Santo et al., 2004; Lucchi et al., 2013a; 2013b). However, in this frame, the alteration of the studied rock samples and the high mobility of elements such as Cs and Rb must be taken into account.

$^{87}Sr/^{86}Sr$ and $^{143}Nd/^{144}Nd$ isotopic ratios measured on the STE 3 rock sample are respectively 0.708129 and 0.512209 (Table 1). Notably, this Sr isotopic ratio is among the lowest values found in the Tuscan Magmatic Province (0.70812-0.71799; Peccerillo, 2005 and references therein); in particular, the $^{87}Sr/^{86}Sr$ isotopic ratio of the Monte Capo Stella dykes is much lower than those of the Orano Porphyry and of the PP-333 mafic enclave (Dini et al., 2002), but it is close to Sr isotopic signature of the HKCA rocks from Capraia Island. The Monte Capo Stella $^{143}Nd/^{144}Nd$ isotopic ratio falls in the general range of TMP (0.51207-0.51234; Peccerillo, 2005 and references therein) and is similar to the Capraia HKCA values (e.g., Conticelli et al., 2009).

DISCUSSION

In the Northern Tyrrhenian Sea and in the Southern Tuscany (inner part of the Northern Apennines chain), silica-rich and mafic magmatic rocks coexist. According to Serri et al. (1993), Bortolotti et al. (2001), Dini et al. (2002), Gagnevin et al. (2004) and Conticelli et al. (2010), they are related to the same geodynamic processes, i.e. the late- to post-orogenic thinning and melting of the lithosphere, occurred in the Neogene-Quaternary times.

Following Poli (1992), the Tuscan mafic magmas originated in the mantle; however, to explain some of their geochemical and isotopic characteristics, closely resembling those of upper crustal rocks, an anomalous contaminated source is invoked. Regarding the composition of these mantle-derived magmas, many authors (e.g., Dini et al., 2002; Poli, 2004; Gagnevin et al., 2004) hypothesised that the more primitive compositions could be represented by the High-K calc-alkaline rocks occurring at Capraia Island and by some MME observed in lavas of the TMP. The ascent of the Tuscan mafic magmas in the thinned crust triggered crustal anatexis and originated highly silicic magmas, emplaced both as unmodified melts or variously modified melts, through the interaction with the mantle magmas (Peccerillo, 2005, with references). Furthermore, the complexity and variety of TMP magmas require the interplay of successive several evolutionary petrogenetic processes.

The interaction of sub-crustal and anatectic felsic magmas is evident in some Elba Island rocks (e.g., Monte Capanne pluton, San Martino porphyry, Orano Porphyry). They display clear evidence of magmatic hybridation processes (Poli et al., 1984; Poli, 1992; Serri et al., 1993; Westerman et al., 2003) such as 1) occurrence of MME in the main granitoid bodies (i.e. Monte Capanne pluton) and dykes (Orano Porphyry), 2) relics of mafic phases (e.g., clinopyroxene, olivine) in disequilibrium with the felsic components, 3) plagioclase of bimodal composition, rounded and embayed quartz phenocrysts and resorption rims in the K-feldspar phenocrysts, 4) "Rapakivi" texture (generally referred to magma mixing process; e.g., Hibbard, 1981; Gagnevin et al., 2004; 2005) of the K-feldspar phenocrysts (e.g., in the Monte Capanne pluton), 5) Sr isotopic disequilibrium between feldspar phenocrysts and the host whole rock.

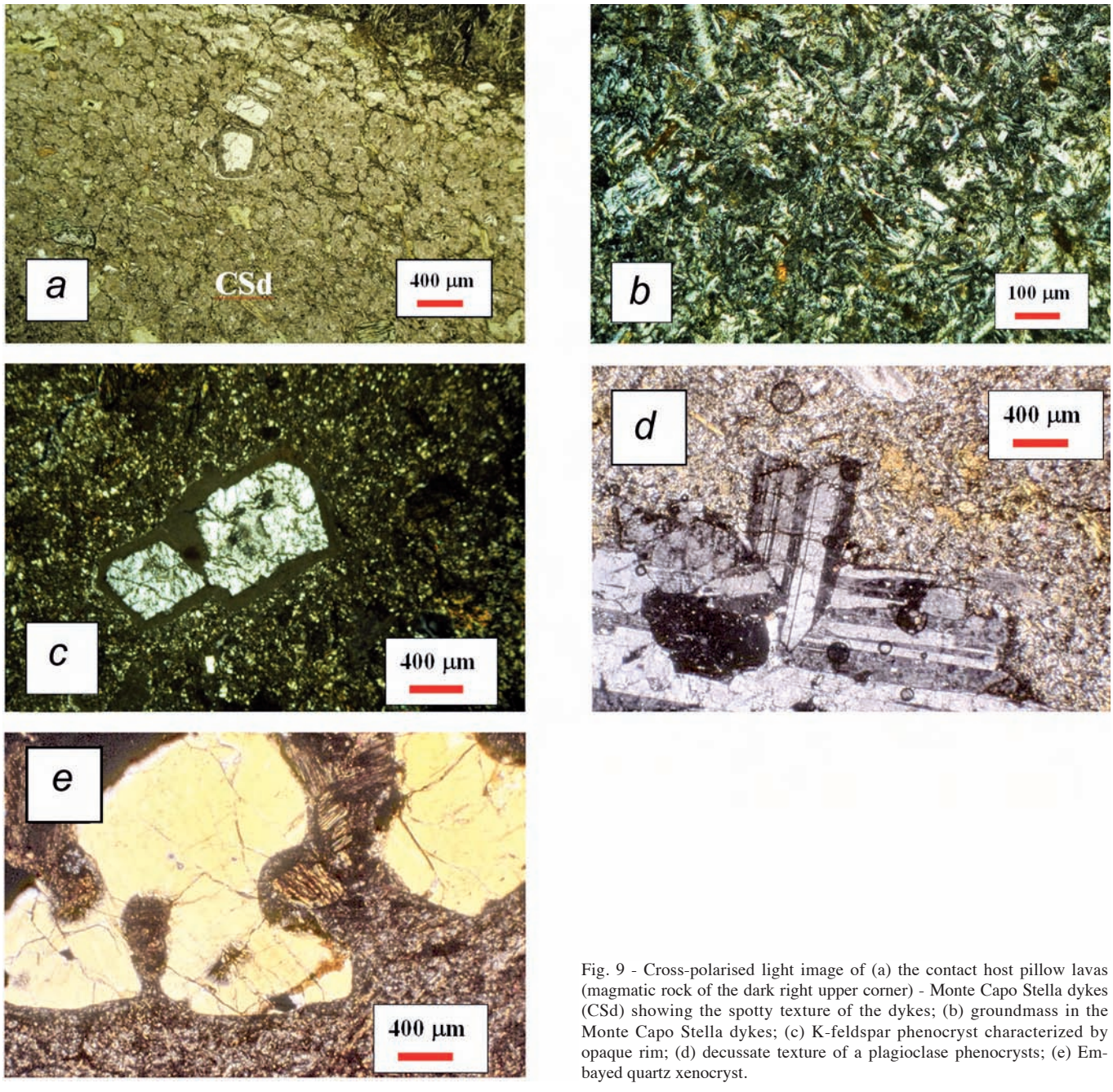

Fig. 9 - Cross-polarised light image of (a) the contact host pillow lavas (magmatic rock of the dark right upper corner) - Monte Capo Stella dykes (CSd) showing the spotty texture of the dykes; (b) groundmass in the Monte Capo Stella dykes; (c) K-feldspar phenocryst characterized by opaque rim; (d) decussate texture of a plagioclase phenocrysts; (e) Embayed quartz xenocryst.

Among the magmatic products of the Elba Island, the Monte Capo Stella dykes display peculiar petrographic and geochemical characteristics. These dacitic dykes fall (Fig. 10a) into the overall compositional field of the Orano Porphyry (cfr. Fig. 5 in Dini et al., 2002), but the Sr isotope ratio is significantly different. The studied dykes differ from the other dykes of eastern Elba (e.g., the quartz-dioritic Casa Carpini dykes, in Pandeli et al., 2006, the mafic shoshonitic Monte Castello dyke in Conticelli et al., 2001) confirming the high compositional variability of the magmatic products in the Elba Island.

In particular, the overall petrographic and compositional data obtained on the MCSD put them within the intermediate-acid rocks of the TMP (Poli, 2004). The compositional characteristics of the dykes, including: a) the wide range of textures and compositions of plagioclase, testifying disequilibrium processes, b) the turbid and resorbed plg crystals (Ab 85-99%) of possible xenocrystic origin, c) the K-feldspar often mantling the plagioclase phenocrysts ("anti-Rapakivi" texture), d) the characteristics of the chondrite-normalised REE and mantle-normalised trace element patterns, and e) the Sr radiogenic ratio, clearly suggest a complex genesis and evolutionary history for this magmatic body.

The studied dacitic dykes have calc-alkaline affinity; they show some compositional analogies with the HKCA Capraia rocks and display REE and trace element patterns very similar to those of the mafic enclave PP-333 collected in the Orano Porphyry. Similar mafic enclaves are commonly found in the silicic Tuscany rocks; they display variable trace element and isotopic signatures reflecting, in several cases, equilibration with the host rocks. However, as noticed by Poli et al. (2002), some of them display patterns of incompatible elements closely resembling those of calc-alkaline rocks from Capraia Island. As a consequence, these

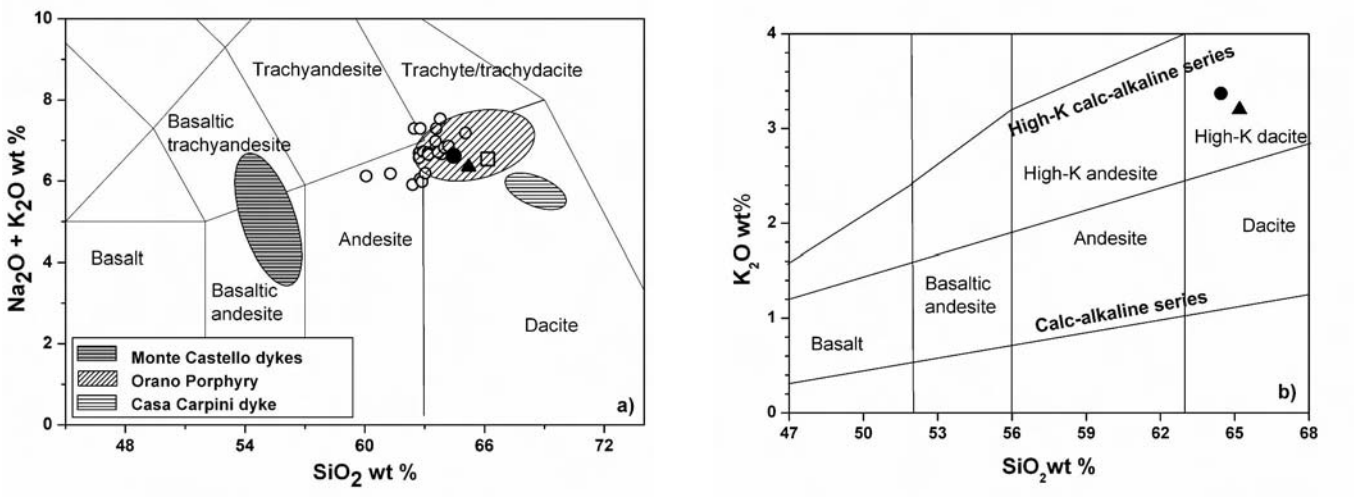

Fig. 10 - (a) Alkali-silica classification diagram (Le Bas et al., 1986) for the Monte Capo Stella dykes (solid circle and triangle); for comparison, Monte Castello and Casa Carpini dykes, Orano Porphyry, MME (PP-333 - open square) and HKCA Capraia rock (open circles) compositions are reported; (b) K_2O-SiO_2 classification (Peccerillo and Taylor, 1976) for the Monte Capo Stella dykes. Symbols as in Fig. 10a. Chemical data are plotted on water-free basis. Data source: Monte Castello dykes - Conticelli et al., 2001; Casa Carpini dykes - Pandeli et al., 2006; Orano Porphyry rocks and enclaves - Dini et al., 2002; Capraia rocks - Prosperini, 1993 and Conticelli et al., 2009.

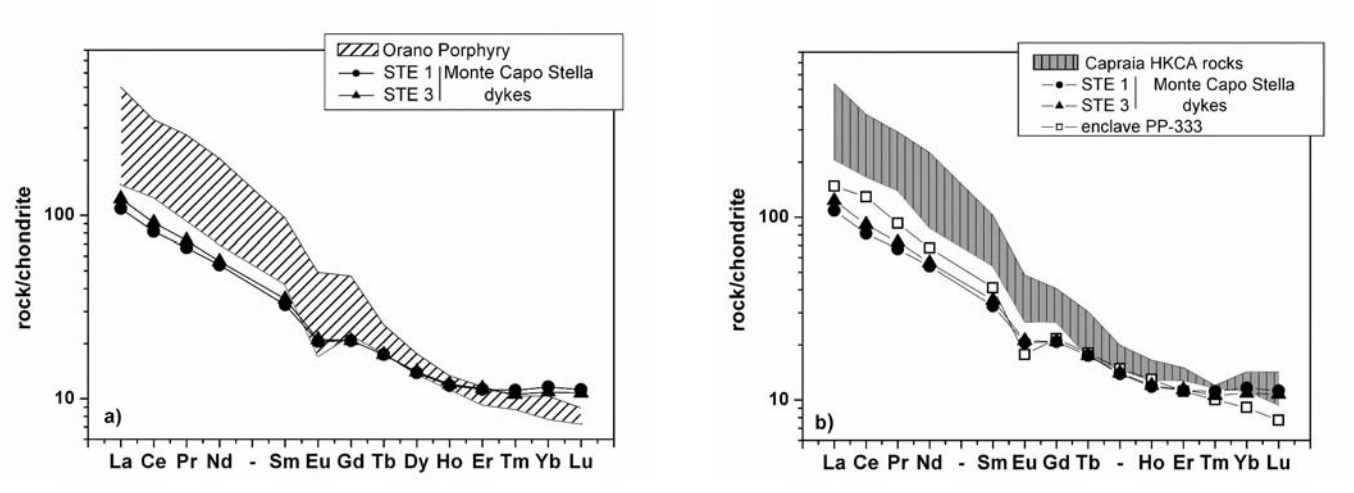

Fig. 11 - Chondrite-normalised REE pattern for the Monte Capo Stella rocks. Patterns for Orano Porphyry (a) and MME (PP-333) and HKCA Capraia rocks, (b) are reported for comparison. Normalisation values from McDonough and Sun (1995). Data source: Orano Porphyry rocks and enclave PP-333 - Dini et al., 2002; Capraia rocks - Prosperini, 1993 and Conticelli et al., 2009.

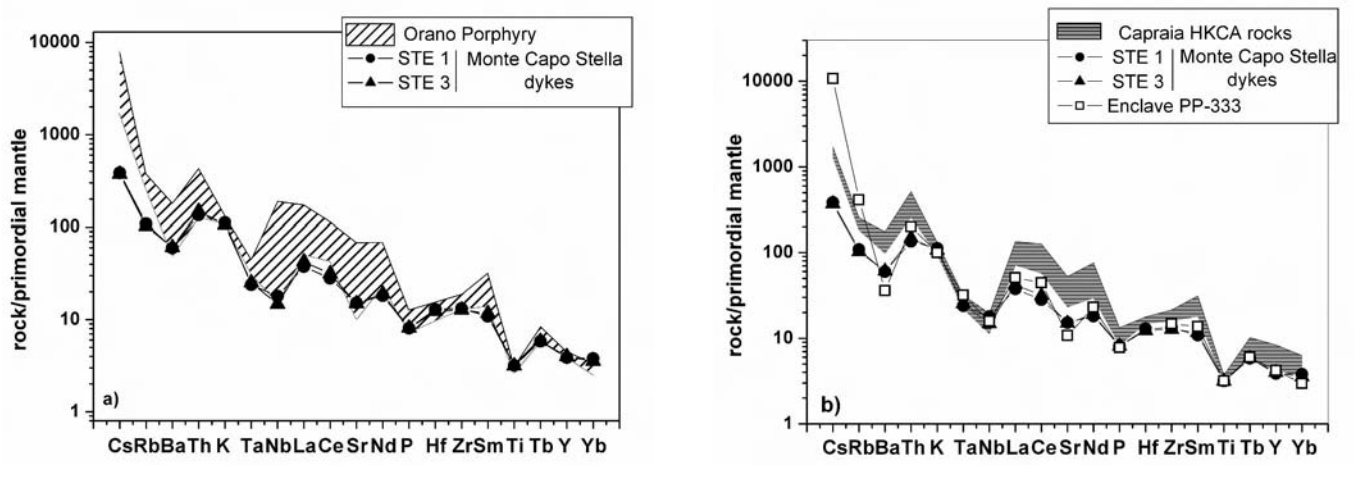

Fig. 12 - Mantle-normalised trace element patterns for the Monte Capo Stella rocks. Patterns for Orano Porphyry (a) and MME (PP-333) and HKCA Capraia rocks (b) are reported for comparison. Normalisation values from Sun and McDonough (1989). Data source: Orano Porphyry rocks and enclave PP-333 - Dini et al., 2002; Capraia rocks - Prosperini, 1993 and Conticelli et al., 2009.

authors hypothesised a calc-alkaline melt as the mafic end member of the Tuscan magmatism. In this framework, thus, the Monte Capo Stella dykes play a relevant role in the study of the Tuscan magmatism and represent the magmatic body, which shows the most peculiar calc-alkaline features in the Elba Island.

All the previously exposed data and considerations lead us to hypothesise for the Monte Capo Stella dykes an initial magma similar to the mafic enclave PP-333 and to HKCA Capraia melt which, in turn, is considered the product of evolved magmas generated in a metasomatised mantle (Poli, 2004). In this way, the Monte Capo Stella dykes, despite the possible interaction with the intruded crustal rocks, represent the first finding of a HKCA rock in the Elba Island.

As concerns the age of the studied dykes, the first attempts to obtain radiometric dating did not give reliable results; however, a Messinian age would be likely hypothesised by the following considerations:

1) In the frame of the intermediate-mafic rocks of the Tuscan Archipelago, the older volcanic and sub-volcanic products are represented by the calc-alkaline volcanites of Capraia Island (7.8-7.2 Ma in Conticelli et al., 2010) and by the plutonic and sub-volcanic rocks of the Elba Island (about 8.0-5.8 Ma in Bortolotti et al., 2001; Dini et al., 2002). In this latter, the magmatic rocks generally show progressively younger age eastward (see Geological Outline). In particular, among the mafic magmatic products, the Orano Porphyry in the western-central Elba (6.8 Ma in Dini et al., 2002) is older than the Monte Castello dyke in the eastern Elba (5.8 Ma in Conticelli et al., 2001).
2) The structural data obtained along the outcrops in the eastern coast of the Capo Stella Promontory (Casa Mazzari locality) indicate that after the emplacement of the Ophiolitic Unit in the tectonic stack of the Elba Island and its partial tectonic elision (see the tectonic superposition of the Nisportino Fm. and Calpionelle limestones above the pillow-lavas), high to medium angle faulting events took place. In particular, this study shows that the MCSD and quartz ± epidote ± chlorite mineralization filled NW-SE trending fractures in the pillow lavas of the Ophiolitic Unit that were locally displaced by a top-to-the- east reverse faulting. Finally, a NW-SE and NE-SW oriented fracturing took place.

In the western-central Elba (including the Monte Capo Stella area), the following succession of events has been reconstructed: firstly, the 8.2-7.4 Ma acidic porphyritic dykes and laccoliths intruded the Ligurian Units (Cretaceous and Tertiary Flysch Units and underlying Ophiolit Unit); successively, the 6.9 Ma Monte Capanne pluton intruded the Ophiolitic Unit and afterwards the 6.8 Ma mafic dykes of Orano Porphyry filled fractures in both the Ligurian Units and Monte Capanne body (Westerman et al., 2000; Bortolotti et al., 2001; Dini et al., 2002, and references therein). Then, at least the Flysch Units were tectonically detached and emplaced to the west and east when the Monte Capanne pluton uplifted. The main eastward detachment surface is particularly evident and known as CEF (Central Elba Fault), active at 6.7 Ma (Maineri et al., 2003). However, Babbini et al. (2001) and Bortolotti et al. (2001) indicated also the existence of other deeper east-verging detachment surfaces, coeval with CEF, in the tectonic pile of central Elba (e.g., Spiaggia del Lido-Valdana-Fosso del Mar dei Carpisi area).

In this frame, also the east-verging (reverse at the outcrop scale) faults, affecting the MCSD, can be likely related to more deep detachments connected to the top-to-the east CEF activity.

Finally, the NW-SE and NE-SW trends of the high-angle lineaments are clearly recognizable in the pre-Zuccale fault systems of the Ophiolitic Unit in the eastern Elba and in the post-Zuccale fault systems of the Porto Azzurro Unit in the Monte Calamita Promontory that downthrown this main detachment fault (Bortolotti et al., 2001; Garfagnoli et al., 2005). In the eastern Elba it is also evident that part of these pre-Zuccale lineaments constituted the pathways for the ascent of the younger, more or less hybridized, mafic magmas (e.g., the 5.8 Ma Monte Castello dyke in the Ophiolitic Unit).

This scenario closely resembles that of the previous emplacement of the Monte Capanne pluton and the younger mafic Orano Porphyry in western Elba, followed by a main eastward tectonic detachment and gliding (i.e. CEF) of the Ligurid cover, due to the final rise of the pluton (cfr. Bortolotti et al., 2001; Dini et al., 2002; Maineri et al., 2003).

According to the above sequence of events, the intrusion of the MCSD can be placed between the intrusion of the 6.8 Ma Orano Porphyry in the western Elba and that of the 5.8 Ma Monte Castello dyke in the eastern Elba. More precisely, taking into account: 1) the top-to-the east, low-middle angle faulting affecting the studied dykes that can be connected with the deep activity of the CEF detachments in the underlying Ophiolitic Units (cfr. Bortolotti et al., 2001) and 2) the intermediate geographic location of the Monte Capo Stella dykes in respect to the other Elba mafic dykes (Orano Porphyry, Monte Castello and Casa Carpini dykes), we suggest for the intrusion of the Monte Capo Stella dykes a possible age of 6.8-6.7 Ma, i.e. between the intrusion of the Orano Porphyry (6.8 Ma) and the CEF activity (6.7 Ma).

CONCLUDING REMARKS

The data obtained in the present study contribute to refine the knowledge of the deformation-evolution of the Ligurian Units and of the complex magmatic framework of the Elba Island. In particular, the new data were useful for the reconstruction of the relationships existing between magmatic intrusions and the final deformations of the tectonic units (e.g., Ophiolitic Unit) in the Island, but also for the improvement of knowledge about the magmatic evolution of the Northern Apennines chain and Tuscan Archipelago. In particular, we would like to remark the following points:

1) The Ophiolitic Unit in the southern Elba Island suffered at least three brittle deformation events after its emplacement and tectonic lamination in the stack of nappes. In particular, the MCSD filled a high angle, NW-SE trending system of fractures and subsequently were affected by top-to-the east, low-middle angle faulting, likely connected to the detachment movements of the CEF. Finally, a high angle, NW-SE and NE-SW fracturing took place and was sealed by Fe oxides and hydroxides;
2) The MCSD are dacitic in composition and can be related to the intermediate magmatism that occurred in the Late Miocene in the Elba Island;
3) The comparison of petrographic and geochemical features of the Monte Capo Stella dykes with other sub-volcanic magmatic bodies of mafic-intermediate composition from the Elba Island point to important differences which confirm the high compositional variability of magmatic products from Elba Island and, in general, of the Tuscan Magmatic Province;

4) The composition of the MCSD displays similarities with that of Capraia HKCA rocks and that of a mafic enclave collected into the Orano Porphyry; so, MCSD shows the clearest calc-alkaline features found in the Elba Island;
5) Field evidence and the above listed considerations point to the emplacement of the MCSD in the time interval between the intrusion of the Orano Porphyry in the western Elba (6.8 Ma) and that of the Monte Castello dyke (5.8 Ma) in the eastern Elba, possibly before the CEF-type detachments activation occurred at 6.7 Ma.

AKNOWLEDGEMENTS

The authors warmly thank E. Saccani (Dipartimento di Fisica e Scienze della Terra, Università di Ferrara, Italy) for providing some preliminary ICP analyses and S. Agostini (Istituto di Geoscienze e Georisorse of Pisa C.N.R. - Italian National Research Council) for providing the Sr and Nd isotopic analyses. The Department of Earth Sciences of the University of Cambridge (UK) is thanked for allowing access to the electron microprobe facility. Thanks are also extended to the referees (Prof. Michele Marroni-University of Pisa and an anonymous Colleague) for improving the manuscript through their corrections and suggestions.

REFERENCES

Avanzinelli R., Elliot T., Tommasini S. and Conticelli S., 2008. Constraints on the genesis of the potassium-rich Italian volcanics from U/Th disequilibrium. J. Petrol., 49:195-223

Avanzinelli R., Lustrino M., Mattei M., Melluso L. and Conticelli S., 2009. Potassic and ultrapotassic magmatism in the circum-Tyrrhenien region: Significance of carbonated pelitic vs. politic sediment recycling at destructive plate margins. Lithos, 113:213-227.

Babbini A., Bortolotti V., Corti S., Dini C., Fazzuoli M., Pandeli E. and Principi G., 2001. Carta geologica dell'Isola d'Elba centrale e orientale, 1:14.500. Ofioliti, 26.

Balestrieri M.L., Pandeli E., Bigazzi G., Carosi R and, Montomoli C., 2011. Age and temperature constraints on metamorphism and exhumation of the syn-orogenic metamorphic complexes of Northern Apennines, Italy. Tectonophysics, 509: 254-271.

Barberi F., Brandi G.P., Giglia G., Innocenti F., Marinelli G., Raggi G., Ricci C.A., Squarci P., Taffi L. and Trevisan L.,1969a. Isola d'Elba, Foglio 126. Carta Geol. d'Italia, Serv. Geol.. d'It., E.I.R.A., Firenze, Italy.

Barberi F., Dallan L., Franzini M., Giglia G., Innocenti F., Marinelli G., Raggi R., Ricci C.A., Squarci P., Taffi L. and Trevisan L.,1967. Carta geologica dell'Isola d'Elba, 1:25.000. E.I.R.A., Firenze, Italy; Ofioliti, 26.

Barberi F., Dallan L., Franzini M., Giglia G., Innocenti F., Marinelli G., Raggi R., Squarci P., Taffi L. and Trevisan L., 1969b. Note illustrative della Carta Geologica d'Italia 1:100.000, Foglio 126 (Isola d'Elba). Serv. Geol. d'It., 32 pp.

Bartole R. 1995. The North Tyrrhenian-Northern Apennines post-collisional system: constraints for geodynamic model. Terra Nova, 7:7-30.

Boccaletti M. and Guazzone G., 1972. Gli archi appenninici, il Mar Ligure ed il Tirreno nel quadro della tettonica dei bacini marginali di retro-arco. Mem. Soc. Geol. It., 11: 201-216.

Bortolotti V., Fazzuoli M., Pandeli E., Principi G., Babbini A. and Corti S., 2001. Geology of the central and eastern Elba Island, Italy. Ofioliti. 26: 97-150.

Bouillin J.P., Poupeau G. and Sabil N., 1994. Etude thermochronologique de la dénudation du pluton du Monte Capanne (Ile d'Elbe, Italie) par les traces de fission. Bull. Soc. Géol. Fran., 165: 19-25.

Carta Geologica d'Italia alla scala 1:50.000, foglio 316, 317, 328, 329 Isola d'Elba. Ispra, Roma (in progress)

Collettini C. and Holdsworth R.E., 2004. Fault zone weakening and character of slip along low-angle normal faults: Insights from the Zuccale Fault, Elba, Italy. J. Geol. Soc. London, 161:1039-1051.

Conticelli S., Bortolotti V., Principi G., Laurenzi M.A., D'Antonio M. and Vaggelli G., 2001. Petrology, mineralogy and geochemistry of a mafic dyke from Monte Castello, Elba Island, Italy. Ofioliti, 26: 249-262.

Conticelli S., Carlson R.W., Widow E. and Serri G., 2007. Chemical and isotopic composition (Os, Pb, Nd, and Sr) of Neogene to Quaternary calc-alkalic, shoshonitic, and ultrapotassic mafic rocks from the Italian peninsula: Inferences on the nature of their mantle sources. In: L. Beccaluva, G. Bianchini and M. Wilson (Eds.), Cenozoic Volcanism in the Mediterranean area. Geol. Soc. Am. Spec. Pap., 418: 171-202.

Conticelli S., Guarnieri L., Farinelli A., Mattei M., Avanzinelli R., Bianchini G., Boari E., Tommasini S., Tiepolo M., Prelevic D. and Venturelli G., 2009. Trace elements and Sr-Nd-Pb isotopes of the western Mediterranean region: Genesis of ultrapotassic to cal-alkaline magmatic associations in a post-collisional geodynamic setting. Lithos, 107: 68-92.

Conticelli S., Laurenzi M., Giordano G., Mattei M., Avanzinelli R., Melluso L., Tommasini S., Boari E., Cifelli F. and Perini G., 2010. Leucite-bearing (kamafugitic/leucititic) and -free (lamproitic) ultrapotassic rocks and associated shoshonites from Italy: constraints on petrogenesis and geodynamics. In: M. Beltrando, A. Peccerillo, M. Mattei, S. Conticelli C. and Doglioni (Eds.), The geology of Italy: tectonics and life along plate margins. J. Virtual Expl., Electr. Ed., ISSN 1441-8142, 36, 20, doi:10.3809/jvirtex.2010.00251.

Daniel J.M. and Jolivet L., 1995. Detachment faults and pluton emplacement: Elba Island (Tyrrhenian Sea). Bull. Soc. Geol. Fran., 166: 341-354.

Dini A., Innocenti F., Rocchi S., Tonarini S. and Westermam D.S., 2002. The magmatic evolution of the late Miocene laccolith-pluton-dyke granitic complex of Elba Island, Italy. Geol. Mag., 139: 257-279.

Dini A., Innocenti F., Rocchi S., Tonarini S. and Westermam D.S., 2006. The Late Miocene Christmas-tree laccolith complex of the Island of Elba. In: G. Pasquarè and C. Venturini (Eds.), Mapping geology of Italy, Firenze, p. 249-258.

Ferrara G. and Tonarini S., 1993. L'Isola d'Elba: un laboratorio di geocronologia. Mem Soc. Geol. It., 49: 227-232.

Gagnevin D., Daly J. and Poli G., 2004. Petrographic, geochemical and isotopic constraints on magma dynamics and mixing in the Miocene Monte Capanne monzogranite (Elba Island, Italy). Lithos, 78: 157-195.

Gagnevin D., Daly J., Poli G. and Morgan D., 2005. Microchemical and Sr isotopic investigation of zoned K-feldspar megacrysts: insights into the petrogenesis of a granitic system and disequilibrium crystal growth. J. Petrol., 46:1689-1724.

Garfagnoli F., Menna F., Pandeli E. and Principi G., 2005. The Porto Azzurro unit (Monte Calamita Promontory, southeastern Elba Island, Tuscany): stratigraphic, tectonic and metamorphic evolution. Boll. Soc. Geol. It., Vol. Spec., 3:119-138.

Hibbard M.J.,1981. The magma mixing origin of mantled feldspars. Contrib. Mineral. Petrol., 76:158-170.

Jolivet L., Faccenna C., Goffé B., Mattei M., Rossetti F., Brunet C., Storti F., Funiciello R., Cadet J.P., D'Agostino N. and Parra T., 1998. Mid crustal shear zones in postorogenic extension: example from the northern Tyrrhenian Sea. J. Geophys. Res., 103: 12123-12160.

Juteau M., Michard A., Zimmermann J.L. and Albarede F., 1984. Isotopic heterogeneities in the granitic intrusion of Monte Capanne (Elba Island, Italy) and dating concepts. J. Petrol., 25: 532-545.

Leake B.E., Woolley A.R., Arps C.E.S., Birch W.D., Gilbert M.C., Grice J.D., Hawthorne F.C., Kato A., Kisch H.J., Krivovichev V.G., Linthout K., Laird J., Mandarino J.A., Nickel E.H., Rock

N.M.S., Schmacher J.C., Smith D.C., Stephenson N.C.N., Ungaretti L., Whittaker E.J.W. and Youzhi G., 1997. Nomenclature of amphiboles: report of the subcommittee on amphiboles of the international mineralogical association, commission on new minerals and mineral namese Can. Mineral., 35: 219-246.

Le Bas M.J., Le Maitre R.W., Streckeisen A. and Zanettin B., 1986. A chemical classification of volcanic rocks based on the Total Alkali-Silica Diagram. J. Petrol., 27 (3): 745-750.

Lippolt H., Wernicke R.S. and Bahr R., 1995. Paragenetic specularite and adularia (Elba, Italy): Concordant (U+Th)-He and K-Ar ages. Earth Planet. Sci. Lett., 132: 43-51.

Lucchi F., Gertisser R., Keller J., Forni F., De Astis G. and Tranne C.A., 2013a. Eruptive history and magmatic evolution of the Island of Salina (central Aeolian Archipelago). In: F. Lucchi, A. Peccerillo, J. Keller, C.A. Tranne and P.L. Rossi (Eds.), The Aeolian Islands volcanoes. Geol. Soc. London Mem., 37: 155-212.

Lucchi F., Santo A.P., Tranne C.A., Peccerillo A. and Keller J., 2013b. Volcanism, magmatism, volcano-tectonics and sea-level fluctuations in the geological history of Filicudi (western Aeolian Archipelago). In: F. Lucchi, A. Peccerillo, J. Keller, C.A. Tranne and P.L. Rossi (Eds.), The Aeolian Islands volcanoes. Geol. Soc. London Mem., 37: 113-154.

Maineri C., Benvenuti M., Costagliola P., Dini A., Lattanti P., Ruggieri G. and Villa I.M., 2003. Sericitic alteration at the La Crocetta depositis (Elba Island, Italy): interplay between magmatism, tectonic and idrotermal activity. Mineral.Dep., 38: 67-86.

Maliverno A. and Ryan W.B.F.,1986. Extention in the Tyrrhenian Sea and shortening in the Apennines as result of arc migration driven by sinking of the lithosphere. Tectonics, 5: 227-245.

Marinelli G., 1959. Le intrusioni terziarie dell'Isola d'Elba. Atti Soc. Toscana Sci. Nat., Serie A, 46: 50-253.

Marinelli G., 1961. Genesi e classificazione delle vulcaniti recenti toscane. Atti Soc. Toscana Sci. Nat., Serie A, 68: 74-116

McDonough W.F. and Sun S.S., 1995. The composition of the Earth. Chem. Geol., 120: 223-253.

Pandeli E., Santo A.P., Morelli M. and Orti L., 2006. Petrological and geochemical data of porphyritic dykes from the Capo Arco Area (Eastern Elba Island, Northern Tyrrhenian Sea). Per. Mineral., 75 (2-3): 241-254.

Patacca E. and Scandone P., 1989. Post-Tortonian mountain building in the Apennines. The role of the passive sinking of a relic lithospheric slab. In: A. Boriani, M. Bonafede, G.B. Piccardo and G.B. Vai (Eds.), The lithosphere in Italy. Advances in Earth science research. Atti Conv. Lincei, 80:157-176.

Peccerillo A., 2005. Plio-Quaternary volcanism in Italy. Petrology, geochemistry, geodynamics. Springer, Heidelberg, p. 315.

Peccerillo A. and Donati S., 2003. The Tuscan Magmatic Province. In: Miocene to Recent plutonism and volcanism in the Tuscan Magmatic Province (central Italy), Per. Mineral., Spec. Iss., 72: 27-39.

Peccerillo A. and Taylor S.R., 1976. Geochemistry of Eocene calc-alkaline rocks from Kastamonu area, Northern Turkey. Contrib. Mineral. Petrol., 58: 63-81.

Peccerillo A., Conticelli S. and Manetti P., 1987. Petrological characteristics and genesis of the recent magmatism of South Tuscany and North Latium. Per. Mineral., 56: 167-183.

Peccerillo A., Poli G. and Serri G., 1988. Petrogenesis of orenditic and kamafugitic rocks from Central Italy. Can. Mineral., 26: 45-65.

Pertusati P.C., Raggi C., Ricci C.A., Duranti S. and Palmeri R., 1993. Evoluzione post-collisionale dell'Elba centro-orientale. Mem. Soc. Geol. It., 49: 223-312.

Petrone C.M., 2010. Relathionship between monogenetic magmatism and stratovolcanoes in western Mexico: the role of low-pressure magmatic processes. Lithos, 119: 585-606.

Poli G., 1992. Geochemistry of Tuscan Archypelago granitoids, Central Italy: the role of hybridization and accessory phases crystallization in their genesis. J. Geol., 100: 41-56.

Poli G., 2004. Genesis and evolution of Miocene-Quaternary intermediate-acidic rocks from the Tuscan Magmatic Province. Per. Mineral., 73: 187-214.

Poli G. and Peccerillo A., 2003. Lamproitic rocks from the Tuscan Magmatic Province. In: Miocene to Recent Plutonism and Volcanism in the Tuscan magmatic province (central Italy). Per. Mineral., Spec. Iss., 72: 225-231.

Poli G., Frey F.A. and Ferrara G., 1984. Geochemical characteristics of the South Tuscany (Italy) volcanic province: constraints on lava petrogenesis. Chem. Geol., 43: 203-221.

Poli G., Peccerillo A., Donati C., 2002. The Plio-Quaternary acid magmatism of Southern Tuscany. In: R.M. Barchi, S. Cirilli and G. Minelli (Eds.), Geological and geodynamic evolution of the Appennines. Boll. Soc. Geol. It., Spec Vol 1: 143-151.

Poli G., Perugini D., Rocchi S. and Dini A., 2003. Miocene to Recent plutonism and volcanism in the Tuscan Magmatic Province. Per. Mineral., Spec. Iss., 72: 27-39.

Principi G., Bortolotti V., Pandeli E., Fanucci F., Chiari M., Dini A., Fazzuoli M., Menna F., Moretti S., Nirta G. and Reale V., con contributi di D'Orefice M. e Graciotti R., (in progress). Note Illustrative della Carta Geologica d'Italia alla scala 1:50.000 foglio 316, 317, 328, 329 Isola d'Elba.

Prosperini N., 1993. Petrologia e geochimica delle rocce di Capraia (Arcipelago Toscano, Italia): un vulcano calcalcalino di origine complessa. BSci. Thesis, Univ. Perugia, Italy.

Rocchi S., Westerman D.S., Dini A., Innocenti F. and Tonarini S., 2002. Two-stage growth of laccoliths at Elba Island, Italy. Geology 30 (11): 983-986.

Santo A.P, Jacobsen S.B. and Baker J., 2004. Evolution and genesis of calc-alkaline magmas at Filicudi volcano, Aeolian Arc (Southern Tyrrhenian Sea, Italy). Lithos, 72: 73-96.

Saupè F., Marignac C., Moine B., Sonet J. and Zimmermann J.L., 1982. Datation par les methodes K/Ar et Rb/Sr de quelques roches de la partie orientale de l'Ile d'Elbe (Province de Livourne, Italie). Bull. Mineral., 105: 236-245.

Serri G., Innocenti F. and Manetti P., 1993. Geochemical and petrological evidence of the subduction of delaminated Adriatic continental lithosphere in the genesis of the Neogene-Quaternary magmatism of central Italy. Tectonophysics, 223: 117-147.

Smith S.A.F., Holdsworth R.E. and Collettini C., 2013. Interactions between low-angle normal faults and plutonism in the upper crust: Insights from the Elba Island. Geol. Soc. Am. Bull., 123 (1/2): 329-346.

Sun S.S. and McDonough W.F., 1989. Chemical and isotopic systematics of oceanic basalts: implications for mantle composition and processes. In: A.D. Saunders and M.J. Norry (Eds.), Magmatism in ocean basins. Geol. Soc. London Spec. Publ., 42: 313-345.

Tanaka T., Togashi S., Kamioka H., Amakawa H., Kagami H., Hamamoto T., Yuhara M., Orihashi Y., Yoneda S., Shimizu H., Kunimaru T., Takahashi K., Yanagi T., Nakano T., Fujimaki H., Shinjo R., Asahara Y., Tanimizu M. and Dragusanu C., 2000. JNdi-1: a neodymium isotopic reference in consistency with LaJolla neodymium. Chem. Geol., 168 (3-4): 279-281.

Tanelli G., Benvenuti M., Costagliola P., Dini A., Lattanzi P., Manieri C., Mascaro I. and Ruggieri G., 2001. The iron mineral deposits of Elba Island: state of the art. Ofioliti, 26: 239-248.

Trevisan L., 1950. L'Elba orientale e la sua tettonica di scivolamento per gravità. Mem. Ist. Geol. Univ. Padova, 16: 5-39.

Trevisan L., 1953. 55ª Riunione Estiva della Società Geologica Italiana. Isola d'Elba, Settembre 1951. Boll. Soc. Geol. It.. 70: 435-472.

Westerman D.S., Dini A., Innocenti F. and Rocchi S., 2003. When and where did hybridization occur? The case of the Monte Capanne pluton, Italy. Atlantic Geol., 39 (2): 147-162.

Westerman D.S., Dini A., Innocenti F. and Rocchi S., 2004. Rise and fall of a nested Christmas-tree laccolith complex, Elba Island, Italy. In: C. Breithunz and N. Petford (Eds.), Physical geology of high-level magmatic systems. Geol. Soc. London Spec. Publ,. 234: 195-213.

Received, July 7, 2014
Accepted, October 30, 2014

APPENDIX

The studied rock samples were previously treated in order to eliminate the effect of seawater impregnation trough repeated washing in distilled water.

Chemical compositions of the mineralogical phases were determined by a Cameca SX100 electron microprobe (EPMA) at the Department of Earth Sciences of the University of Cambridge (UK). The EPMA is equipped with five WDS (wave-length dispersive) mass spectrometers and one EDS (energy-dispersive) spectrometer. The electron microprobe was operated at 15 kV high-voltage and 10 nA beam current for major elements, which was raised up to 100 nA for measuring minor and selected trace elements. Feldspar were analysed using a defocussed 5mm beam size, whereas a focused beam has been used for all other mineral phases. The Cameca XPHi protocol was used to correct matrix effect. Accuracy and analytical precision are the same as reported by Petrone (2010).

Major and trace element analyses of the collected rock samples were carried out at the Activation Laboratories, Ancaster, Ontario, Canada. For major oxides and selected trace elements (Ba, Sr, Y, Zr, Sc, V), samples were prepared and analyzed in a batch system. Each batch contains a method reagent blank, certified reference material and 17% replicates. Samples were mixed with a flux of lithium metaborate and lithium tetraborate and fused in an induction furnace. The molten melt was immediately poured into a solution of 5% nitric acid containing an internal standard, and mixed continuously until completely dissolved (~30 minutes). The samples were run on a combination simultaneous/sequential Thermo Jarrell-Ash ENVIRO II ICP (inductively coupled plasma). Calibration is performed using 7 prepared USGS and CANMET certified reference materials. One of the 7 standards is used during the analysis for every group of ten samples. Detection limit is in the range 0.01 and 0.001 (%) for major elements and between 1 and 5 (ppm) for trace elements. The same sample solution was spiked with internal standards to cover the entire mass range, was further diluted and introduced into a Perkin Elmer SCIEX ELAN 6000,6100 or 9000 ICP/MS (inductively coupled plasma-mass spectrometry) using a proprietary sample introduction methodology. The detection limits in ppm are: Pb = ppm; Ni, Co, Cr, Rb = 1 ppm; Nb = 0.2; Cs, Hf, Ta = 0.1; La, Ce, Nd, Eu, Th = 0.05; Lu = 0.02; Pr, Sm, Gd, Tb, Dy, Ho,Eb, Yb U = 0.01; Eu, Tm = 0.005.

Sr and Nd isotope ratios were measured via TIMS techniques at the Istituto di Geoscienze e Georisorse of Pisa C.N.R. (Italian National Research Council) using a Finnigan MAT 262 multicollector mass spectrometer running in dynamic mode. The measured $^{87}Sr/^{86}Sr$ ratios have been normalised to $^{87}Sr/^{86}Sr = 0.1194$ and $^{143}Nd/^{144}Nd$ ratios to $^{143}Nd/^{144}Nd = 0.7219$. During the measurement period, the mean measured value of $^{87}Sr/^{86}Sr$ for the NIST–SRM 987 standard was 0.710242 ± 0.000013 (2SD, N = 25), while the mean $^{143}Nd/^{144}Nd$ for the La Jolla standard was 0.511847 ± 0.000008 (2SD, N = 25). The JNdi-1 standard (Tanaka et al. 2000) was also analyzed and yielded a $^{143}Nd/^{144}Nd$ value of 0.512100 ± 0.000010 (2SD, N = 25). The total procedure blanks, 0.5 ng and 0.1 ng of Sr and Nd, respectively, were negligible for the analyzed samples.